

## Crops and Soils Research Paper

**Cite this article:** Chirico GB, Pelosi A, De Michele C, Falanga Bolognesi S, D'Urso G (2018). Forecasting potential evapotranspiration by combining numerical weather predictions and visible and near-infrared satellite images: an application in southern Italy. *The Journal of Agricultural Science* **156**, 702–710. <https://doi.org/10.1017/S0021859618000084>

Received: 1 June 2017  
Revised: 15 January 2018  
Accepted: 5 February 2018  
First published online: 28 February 2018

### Key words:

Crop water requirements; Earth observation; forecasting; numerical weather predictions; potential evapotranspiration

### Author for correspondence:

G. B. Chirico, E-mail: [gchirico@unina.it](mailto:gchirico@unina.it)

# Forecasting potential evapotranspiration by combining numerical weather predictions and visible and near-infrared satellite images: an application in southern Italy

G. B. Chirico<sup>1</sup>, A. Pelosi<sup>2</sup>, C. De Michele<sup>3</sup>, S. Falanga Bolognesi<sup>3</sup> and G. D'Urso<sup>1</sup>

<sup>1</sup>Department of Agricultural Sciences, University of Naples Federico II, Portici, Italy; <sup>2</sup>Department of Civil Engineering, University of Salerno, Fisciano, Italy and <sup>3</sup>Ariespace s.r.l., Naples, Italy

## Abstract

Irrigation according to reliable estimates of crop water requirements (CWR) is one of the key strategies to ensure long-term sustainability of irrigated agriculture. In southern Mediterranean regions, during the irrigation season, CWR is almost totally controlled by the potential evapotranspiration of the irrigated crop. An innovative system for forecasting crop potential evapotranspiration (ET<sub>p</sub>) has been implemented recently in the Campania region (southern Italy). The system produces ET<sub>p</sub> forecasts with a lead time of up to 5 days, by coupling the visible and near-infrared crop imagery with numerical weather prediction outputs of a limited area model. The forecasts are delivered to farmers with a simple and intuitive web app interface, which makes daily real-time ET<sub>p</sub> maps accessible from desktop computers, tablets and smartphones. Forecast performances were evaluated for maize fields of two farms in two irrigation seasons (2014–2015). The mean absolute bias of the forecasted ET<sub>p</sub> was <0.3 mm/day and the RMSE was <0.6 mm/day, both for lead times up to 5 days.

## Introduction

Global population growth is determining a progressive increase of the demand for food supply, which in turn increases the amount of water that needs to be allocated for crop production. In some areas of the world, irrigated agriculture represents the major consumer of water resources, typically about 0.70 of the total water use (UNWAP 2016). Indeed, irrigation allows lands to be, on average, twice as productive as rain-fed lands. In areas such as southern Mediterranean regions, irrigation is essential for ensuring high crop yields during late spring and summer, characterized by high temperatures and lack of rain (Wriedt *et al.* 2009).

Improving the efficiency of water use for irrigation is required for ensuring long-term sustainability of irrigated agriculture (Pereira *et al.* 2009). The EU Common Agricultural Policy, combined with the Water Framework Directive, imposes a substantial increase in the efficiency of water use in agriculture for the next decades on farmers and irrigation managers (Heinz 2008).

The strategies for more rational and efficient water consumption in agriculture may be categorized as policy, engineering, system and irrigation/agronomic practice interventions (Stöckle 2001). Among the latter interventions, one possible solution is to irrigate according to reliable estimates of actual water that must be supplied by irrigation to satisfy crop water needs, which are not provided by rainfall or by water available in the profile (Romano *et al.* 2011).

For this purpose, irrigation advisory services have been built to help farmers decide the right amount of water to be supplied. These services provide an assessment of the crop water requirement (CWR) to farmers, accounting for the meteorological conditions and the development stage of the crop. The effectiveness of these CWR estimates relies on the availability of updated data about the crop and the meteorological conditions, with adequate spatial and temporal resolution (Allen *et al.* 2011).

Current Earth observation (EO) systems provide multispectral imagery of crops with relatively high spatial and temporal resolutions. Several models have been developed and successfully applied to exploit the available time series of visible and near-infrared (VIS-NIR) images of the crop for estimating crop potential evapotranspiration (ET<sub>p</sub>) and crop water use. The main space agencies, such as NASA and ESA, provide georeferenced multispectral imagery with a high spatial resolution (30 m or less) and small time intervals (9 days or less), free of charge. This data policy enhanced the development of satellite-based services that can offer irrigation advice to farmers at a reasonable cost. A review of the current application of remote sensing for crop water management has been provided recently by Calera *et al.* (2017).

In southern Mediterranean regions, ET<sub>p</sub> is the main component of CWR, under the assumption that irrigated crops grow under excellent agronomic and soil water conditions (Allen *et al.* 1998). One possible approach for estimating ET<sub>p</sub> is to apply the Penman–Monteith equation,

with crop parameters estimated from remotely sensed images. This is the so-called ‘one-step’ approach followed by some satellite irrigation services, such as IRRISAT in Southern Italy (<https://www.irrisat.com/en/>), EO4Water in Lower Austria (<https://eo4water.com/>) and IRRIEYE in Southern Australia (<http://www.irrieye.com>).

In addition to crop parameters, the Penman–Monteith equation needs meteorological data as input variables, including air temperature, wind speed, solar radiation and relative humidity. These data are often unavailable or available only with large uncertainty, since they are estimated by spatial interpolation of sparse meteorological ground stations. The reliability of meteorological data produced by numerical weather prediction (NWP) models has improved considerably in the 21st century. Thus, NWP model outputs are a valuable source for estimating the meteorological variables relevant for calculating  $ET_p$  maps, alternative to the spatial interpolation of spatially coarse ground-based weather data sets (WMO 2012).

Operational NWP models can be also exploited for forecasting  $ET_p$  a few days ahead. This is particularly relevant for providing irrigation advice to farmers in operative scenarios, since it allows planning of irrigation water supply based on the expected meteorological conditions rather than on past and current meteorological data.

The current study presents an innovative  $ET_p$  forecasting system that has been implemented recently in the Campania region (southern Italy). The forecasting system has been integrated into the IRRISAT irrigation advisory service, which has been operative in the Campania region since year 2007 and was originally based on remote-sensing crop imagery and ground-based meteorological data. The new forecasting system integrates high-resolution numerical weather forecasts with VIS-NIR crop imagery for providing  $ET_p$  maps to farmers with a lead time of 5 days. The current paper presents the methodological background and key operational settings of the forecasting system. The forecast performance of crop  $ET_p$  was evaluated at two experimental sites in Campania region, by comparing the forecasted  $ET_p$  with that estimated by means of ground meteorological observations.

## Materials and methods

### Methodological background for crop potential evapotranspiration assessment

The CWR can be estimated according to the standard approach proposed by Allen *et al.* (1998):

$$CWR = ET_p - P_e \quad (1)$$

where  $ET_p$  (mm) is the crop potential evapotranspiration, i.e. the amount of water consumed by crops via soil evaporation and plant transpiration under optimum soil water conditions, and  $P_e$  (mm) is the effective precipitation, i.e. the part of the rainwater effectively available for crops, namely the rainwater excluding the losses due to run-off and foliage interception.

During the irrigation season in southern Italy, due to features of the Mediterranean climate, rainfall events are rare and generated generally by intense thunderstorms of short duration and small spatial extent, highly influenced by the local topography (Furcolo *et al.* 2016). These rainfall patterns make monitoring difficult with traditional rain gauge networks (Zoccatelli *et al.* 2015), and forecasting with current NWP models is highly uncertain (Montani *et al.* 2011). These characteristics of summer and spring

have been enhanced by the climatic change observed in the last century (Diodato *et al.* 2011). Such rainfall events may cause floods at local scale but provide little water supply to open field crops (Preti *et al.* 2011). Thus, the rainfall contribution to overall CWR is generally negligible as compared with crop  $ET_p$  (D’Urso 2010).

Potential evapotranspiration depends on both crop parameters, such as surface albedo and crop height, and weather variables, such as air temperature, solar radiation, humidity, wind speed and air pressure.

One conventional approach for assessing  $ET_p$  is the so-called ‘two-steps’ procedure recommended by Allen *et al.* (1998). According to this procedure,  $ET_p$  can be evaluated by multiplying the reference evapotranspiration ( $ET_0$ ) with a crop coefficient ( $K_c$ ).

The reference evapotranspiration is the potential evapotranspiration of a hypothetical grass reference crop under optimum soil water conditions and can be calculated with the FAO Penman–Monteith equation using only weather information:

$$ET_0 = \frac{1}{\lambda} \frac{\Delta(R_n - G) + \gamma(900/T + 273)U(e_s - e_a)}{\Delta + \gamma(1 + 0.34U)} \quad (2)$$

where  $\lambda$  is the latent heat of vaporization of water (MJ/kg),  $R_n$  is the net radiation at the crop surface (MJ/m<sup>2</sup>/day),  $G$  is the soil heat flux density (MJ/m<sup>2</sup>/day),  $T$  is the daily mean air temperature at 2 m height (°C),  $U$  is the wind speed at 2 m above the ground (m/s),  $e_s$  is the saturation vapour pressure (kPa),  $e_a$  is the actual vapour pressure (kPa),  $\Delta$  is the slope of the vapour pressure curve (kPa/°C) and  $\gamma$  is the psychrometric constant (kPa/C).

The crop coefficient is then a proxy of the parameters describing the canopy development, i.e. leaf area index (LAI), surface albedo and crop height (Vuolo *et al.* 2015).

An alternative method, which is the one used by IRRISAT for producing remote-sensing-based estimates of  $ET_p$ , is the so-called ‘one-step’ approach (D’Urso & Menenti 1995) that explicitly employs aerodynamic and surface resistances to compute  $ET_p$  as follows:

$$ET_p = \frac{86400}{\lambda} \left[ \frac{\Delta(R_n - G) + \rho c_p(e_s - e_a)/r_a}{\Delta + \gamma(1 + r_s/r_a)} \right] \quad (3)$$

where  $\rho$  is the mean air density at constant pressure (kg/m<sup>3</sup>),  $c_p$  is the specific heat of the air (MJ/kg/°C),  $r_a$  and  $r_s$  are the aerodynamic and surface resistances, respectively (s/m).

Visible and near-infrared imagery are processed to estimate the canopy parameters required for applying Eqn (3): LAI, crop height ( $h_c$ ) and the hemispherically integrated albedo ( $r$ ).

The variability of LAI during the phenological development of the crop has the largest impact on the estimation of  $ET_p$ , as compared with  $r$  and  $h_c$  (Vanino *et al.* 2015).

Leaf area index and  $h_c$  are used for computing the aerodynamic and surface resistances:

$$r_a = \frac{\ln[2 - 2/3h_c/0.123h_c] \ln[2 - 2/3h_c/0.0123h_c]}{(0.41)^2 U} \quad (4)$$

$$r_s = \begin{cases} \frac{200}{LAI} & \forall LAI \leq 4 \\ 50 & \forall LAI > 4 \end{cases} \quad (5)$$

Albedo is used to estimate the fraction of incoming short-wave radiation contributing to the net radiation  $R_n$ .

IRRISAT operationally exploits LANDSAT-8 VIS-NIR imagery for estimating canopy parameters with a spatial resolution of 30 m. Upgrades are planned to exploit the Sentinel-2 remote-sensing imagery with a spatial resolution of 10 m.

The surface reflectance is used to estimate LAI with the CLAIR model (Clevers 1989):

$$\text{LAI} = -\frac{1}{\alpha} \ln \left( 1 - \frac{\text{WDVI}}{\text{WDVI}_{\infty}} \right) \quad (6)$$

where  $\alpha$  is a shape parameter that must be calibrated with LAI field measurements, WDVI is the weighted difference vegetation index and  $\text{WDVI}_{\infty}$  is the asymptotic value for  $\text{LAI} \rightarrow \infty$ , and it is computed from the spectral reflectance (Vuolo *et al.* 2013).

Given the limited spectral resolution of the VIS-NIR imagery employed, albedo is calculated as a weighted sum of surface spectral reflectance:

$$r = \sum_{\lambda=1}^n \rho_{\lambda} w_{\lambda} \quad (7)$$

where  $\rho_{\lambda}$  is the surface spectral reflectance derived from the atmospheric correction, while  $w_{\lambda}$  is the fraction of solar irradiance in each sensor band, according to D'Urso & Calera Belmonte (2006).

Crop height can be derived from crop maps or as function of LAI with a specific regression equation that needs to be empirically determined. When this information is not available,  $h_c$  is fixed to 0.4 m. This is an acceptable approximation since the variability of crop height  $h_c$  has little impact on the value of  $\text{ET}_p$ , especially in southern Mediterranean regions where the aerodynamic term of the FAO Penman–Monteith equation is much smaller than the corresponding radiative term (Vuolo *et al.* 2015).

### Numerical weather forecasts

The new  $\text{ET}_p$  forecasting system implemented by IRRISAT adopts the NWP outputs provided by COSMO-LEPS, which is a Limited Area Ensemble Prediction System, operated by the HydroMeteoClimate Regional Service of Emilia-Romagna, located in Bologna, Italy (ARPA-SIMC). Pelosi *et al.* (2016) showed that COSMO-LEPS produces skilful and reliable forecasts of the weather variables relevant for reference evapotranspiration ( $\text{ET}_0$ ) estimates in Campania region, up to 5 days ahead, with limited sensitivity to the forecast lead time.

Since December 2011, COSMO-LEPS has run twice a day, at 00:00 UTC and 12:00 UTC. The model has a forecast range of 132 h, with data available at 3 h intervals and a spatial resolution of 7.5 km. The relevant weather variables to calculate  $\text{ET}_p$  are extracted from GRIB (GRIdded Binary or General Regularly-distributed Information in Binary form) files released as output of the 00:00 UTC run: atmospheric pressure reduced to mean sea level, net short-wave radiation, albedo, wind speed at 10 m above ground level, temperature and relative humidity at 2 m. Figure 1 shows the points of the numerical grid adopted by COSMO-LEPS covering the Campania region.

The numerical weather forecasts at a specific site are retrieved by a triangle-based bi-linear interpolation method, which consists of interpolating the three numerical grid points closest to the examined site. A statistical post-processing technique is applied for partially removing systematic and non-systematic forecast errors produced by the NWP models, when ground measurements of weather variables are available (Pelosi *et al.* 2017).



**Fig. 1.** COSMO-LEPS numerical grid (red circles) over Campania region and location of Improsta and Soffritti farms hosting the verification sites.

### Web2.0 service for delivering crop potential evapotranspiration forecast maps

Farmers can access  $\text{ET}_p$  forecast maps by means of a dedicated web-based platform with a protected login. At first access, farmers need to draw the boundary of plots for which they request the advisory service on a base layer. The platform then displays updated maps and time series of crop LAI and daily crop evapotranspiration, with a forecast horizon up to 5 days, beside other variables of potential interest for the farmer (e.g. air temperature, rainfall, etc.). By clicking on the maps, the platform displays the time series of the corresponding variables, either for each selected pixel or aggregated at plot scale, according to the user requirement.

Sample layouts of the windows dedicated to LAI and crop  $\text{ET}_p$  are displayed in Figs 2 and 3. The web layouts are made up of a coloured map with a legend, and graphs displaying both the current value and the time series of the selected variable. In case of  $\text{ET}_p$  time series, the graph provides the values 5 days ahead of the current day. Users can move the map by keeping the mouse button held down while dragging it, and can use the zoom in and zoom out button in the top left corner of the map. For touchscreen devices, users can also use the multi-touch gesture to pan and zoom the map. The position button, on the bottom left, displays your location (based on global position system (GPS) device of tablet or smartphone) on the map. Data in tabular format are also provided as a summary report.

### Measurements at the experimental maize fields

The test sites consisted of maize crop fields hosted by two farms, Soffritti (40°27') and Improsta (15°1'), located in the Campania region (Fig. 1). Under the Köppen–Geiger climate classification, this region is characterized by dry-summer sub-tropical climates, which are often referred to as Mediterranean climate. During summer, the mean monthly temperature ranges from 25 to 30 °C and during winter, between 11 and 17 °C. The precipitation patterns are influenced strongly by the interaction of wet air masses with the orography (Pelosi & Furcolo 2015): mean annual

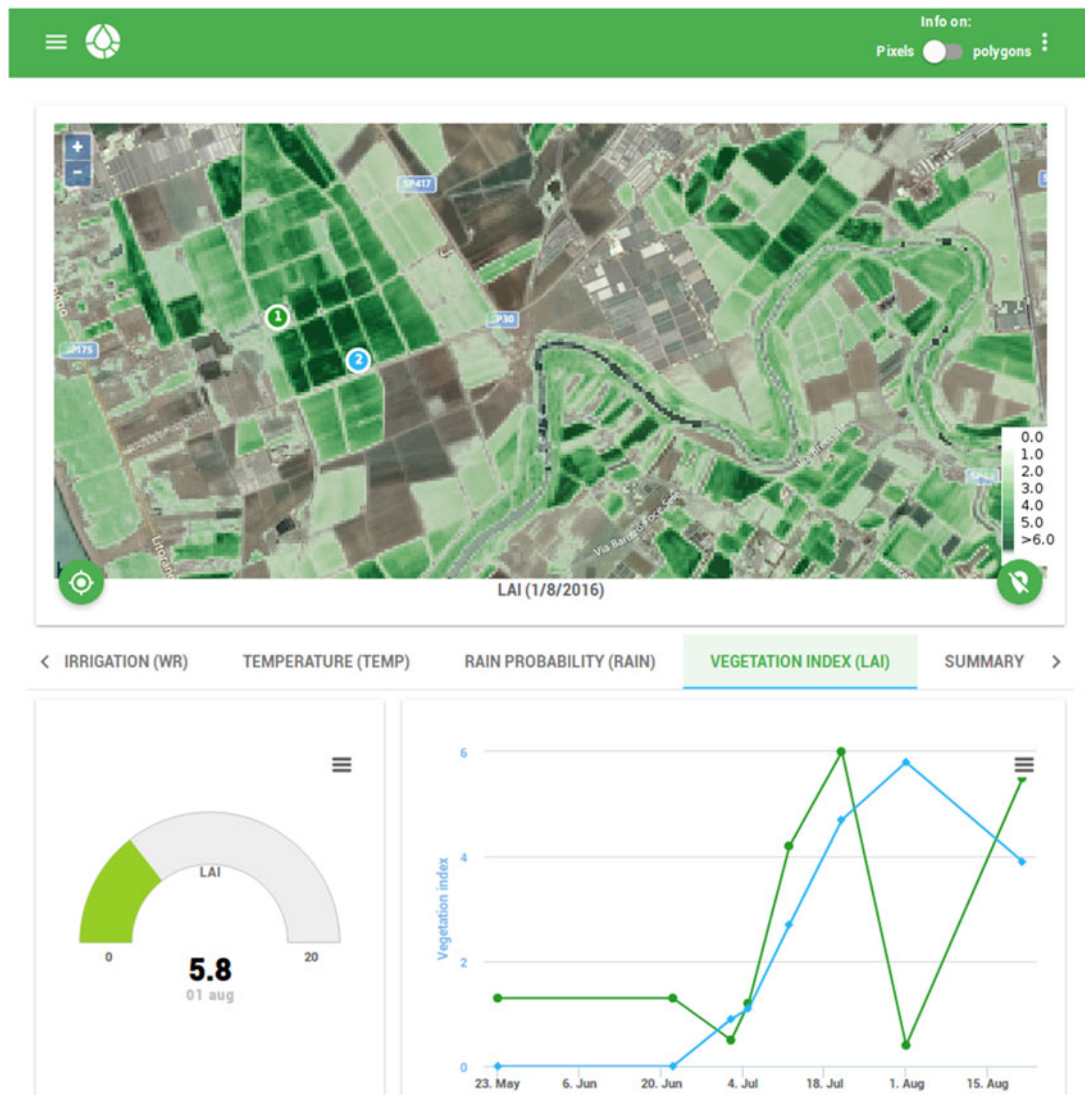


**Fig. 2.** Layout of the web-based app, displaying LAI map and time series at a farm plot: a coloured map with legend is located at the top. The graph at the bottom left displays the LAI value at the current day. On the bottom right, the graph displays the time series of the LAI.

precipitation ranges from 800 to 1100 mm. The maximum monthly precipitation values are recorded during November and December, minimum values during July and August. Irrigation in open fields starts no earlier than April and lasts until the end of September, although the actual time span of the irrigation season is influenced by climatic fluctuations and specific agricultural practices.

The two selected farms are representative of two different topographic conditions: Improstata is located in a large floodplain; Soffritti is located in a hilly inland area. Choosing different terrain is relevant for evaluating  $ET_p$  forecast performances, since local topographic conditions significantly affect the reliability of the numerical weather forecast, as in other coastal regions of the central Mediterranean basin (Buzzi *et al.* 1994), as well as of satellite-based estimations of LAI (Calera *et al.* 2017).

Each farm was equipped with ground-based automatic weather stations (AWS) providing measurements of precipitation, atmospheric pressure, solar radiation, relative humidity, wind speed at 10 m above ground level and temperature at 2 m, with high accuracy and precision standards.

Ground LAI measurements were taken as follows: from seven fields at Improstata on two dates in 2014, simultaneously to DEIMOS-1 satellite acquisitions; from six fields at Soffritti farm on eight dates in 2015, some of them close to or at the same time as LANDSAT-8 Operational Land Imager (OLI) satellite acquisitions.

Ground non-destructive measurements of LAI and leaf mean tilt angle were made with a LICOR LAI-2000 Plant Canopy Analyser (LI-COR 1992), which works by comparing the intensity of diffuse incident illumination measured at the bottom of the canopy with that arriving at the top. In order to reduce the effect of multiple scattering on LAI-2000 measurements, the instrument was only operated near dusk and dawn (6:30–9:30 a.m.; 6:30–8:30 p.m.) under diffuse radiation conditions, using one sensor for both above- and below-stand measurements. In order to prevent interference caused by the operator's presence and the illumination conditions, the sensor field of view was limited using a 180° view cap. Measurements were azimuthally oriented opposite to the sun azimuth angle. Leaf area index measurements were taken with the instrument held a few centimetres above the soil,

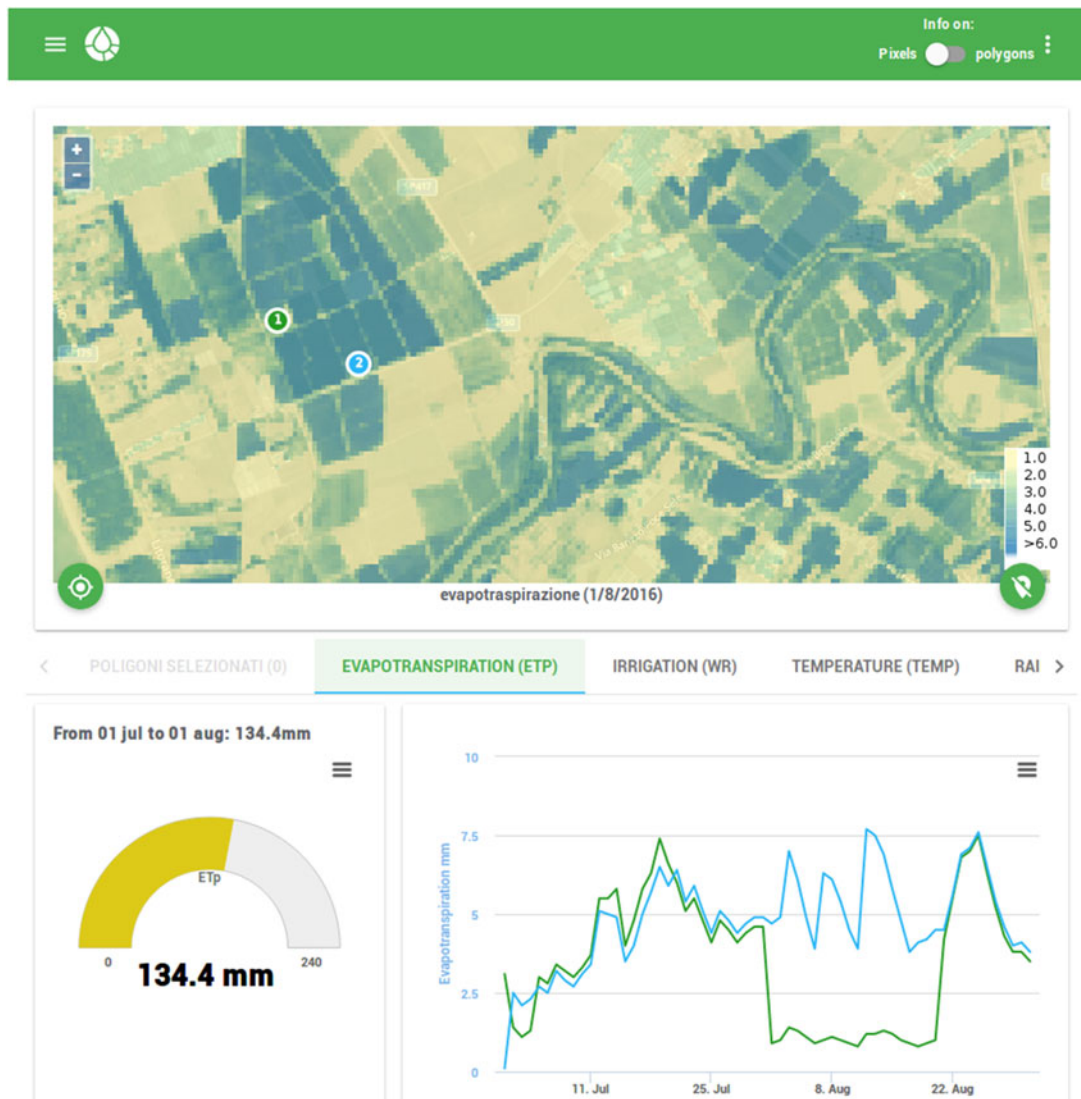


**Fig. 3.** Layout of the web-based app, displaying crop  $ET_p$  map and time series at a farm plot: a coloured map with legend is located at the top. The graph at the bottom left displays the cumulative  $ET_p$  with a user-defined time interval. On the bottom right, the graph displays the time series of the cumulative  $ET_p$ .

generally within 3 days of image data acquisition. A measurement of ambient light was made with the sensor extended upward and over the top of the canopy at arm's length. Eight below-canopy readings were then made. This procedure was conducted three times per spot, and the resulting 24 samples comprise one full set of measurements. Finally, each centre of the LAI-2000 transacts was geolocated using GPS measurements. This measurement protocol allowed determination of statistically meaningful LAI values, characterized by a low ratio between the standard error of the LAI (SEL) and LAI itself (SEL/LAI ranged between  $\approx 0.03$  and  $\approx 0.13$  for the test sites at Improsta and SEL/LAI ranged between  $\approx 0.02$  and  $\approx 0.17$  for the test sites at Soffritti); thus, the actual LAI should be within 11% of the LAI sample mean.

Leaf area index maps at Improsta were derived by combining DEIMOS-1 satellite acquisitions with a spatial resolution of 22 m and LANDSAT-8 imagery, to get LAI data with an average time frequency of 1 week. Leaf area index maps at Soffritti were derived with a spatial resolution of 30 m from LANDSAT-8 imagery elaborated with a time frequency of 15 days, allowing for favourable atmospheric conditions.

DEIMOS-1 is a commercial tasking EO satellite and is part of the Disaster Monitoring Constellation (DMC) (<http://www.dmcii.com>). The sensor records radiance in three spectral bands corresponding to green (520–600 nm), red (630–690 nm) and near-infrared (770–890 nm) parts of the electromagnetic spectrum at a ground sampling distance (GSD) of 22 m. DEIMOS-1 images were processed to a high degree of accuracy using an industry-standard atmospheric correction algorithm (ATCOR-2) (Richter 1996; GEOSYSTEMS 2017).

LANDSAT-8 OLI data at a GSD of 30 m were generated routinely by the Landsat Ecosystem Disturbance Adaptive Processing System (LEDAPS) and obtained through the USGS Land Science Research and Development (LSRD) website; LEDAPS uses Dense Dark Vegetation (DDV) targets to estimate the aerosol optical thickness (AOT). The estimated AOT was used afterwards as input to the Second Simulation of a Satellite Signal in the Solar Spectrum (6S) radiative transfer model.

All images were elaborated using Eqn (6) with  $\alpha = 0.35$ , which was determined for this area based on previous field campaigns (D'Urso & Calera Belmonte 2006).

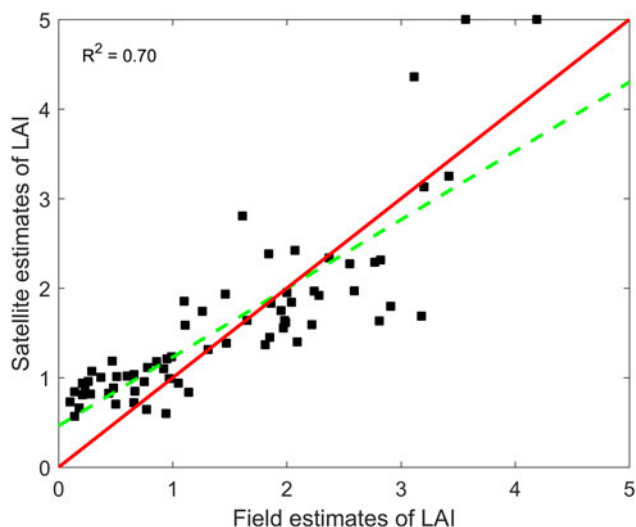


**Fig. 4.** Scatter plot of satellite estimates of LAI v. field estimates of LAI at Improsta and Soffritti farms. The red line is the 45-degree line of perfect agreement between the two estimates; the green dashed line is the least-squares line computed from data. The  $R^2$  statistics refers to the perfect agreement between the two data sets.

**Results**

*Satellite-based estimates of leaf area index*

In total, 62 ground LAI measurements (seven fields per two dates at Improsta and six fields per eight dates at Soffritti) were taken during the two irrigation seasons 2014 and 2015. The satellite estimations were in good agreement with the ground observations (coefficient of determination  $R^2 = 0.70$ ). Figure 4 shows the

scatterplot of field and satellite LAI estimates of years 2014 and 2015 at the test sites.

Figure 5 shows the time evolution of satellite and field LAI estimates at the three test fields at Improsta and Soffritti, respectively. The data show good agreement in the central part of the irrigation season, while larger differences are observed in the second half of July. A systematic overestimation of LAI by satellite was observed at some plots in Soffritti. The impact of these differences on  $ET_p$  forecasts was generally negligible, especially for high LAI values, given the asymptotic behaviour of Eqn (3).

Potential evapotranspiration prediction errors obtained by applying Eqn (3) with LAI equal to the one estimated with the last satellite acquisition were generally larger than those obtained by applying Eqn (3) with LAI estimated by remote-sensing, especially in the central part of phenological development of the crop.

*Crop potential evapotranspiration forecasts*

The performances of the new  $ET_p$  forecasting system implemented in IRRISAT at the selected fields are presented. The ‘best estimate’ of  $ET_p$ , taken as a benchmark to assess the forecast performances, was computed by using ground-based weather data combined with interpolated values of LAI between two satellite estimates. The IRRISAT approach used COSMO-LEPS forecasts for weather variables and LAI equal to the last available satellite estimate, to provide forecasts of  $ET_p$  with a lead time of up to 5 days.

The performance analysis also included a ‘mixed approach’, which used COSMO-LEPS weather forecasts and interpolated values of LAI between two satellite estimates, to evaluate the impact of IRRISAT LAI approximation on  $ET_p$  forecasts. Table 1 provides a summary of the methods employed in this comparison study.

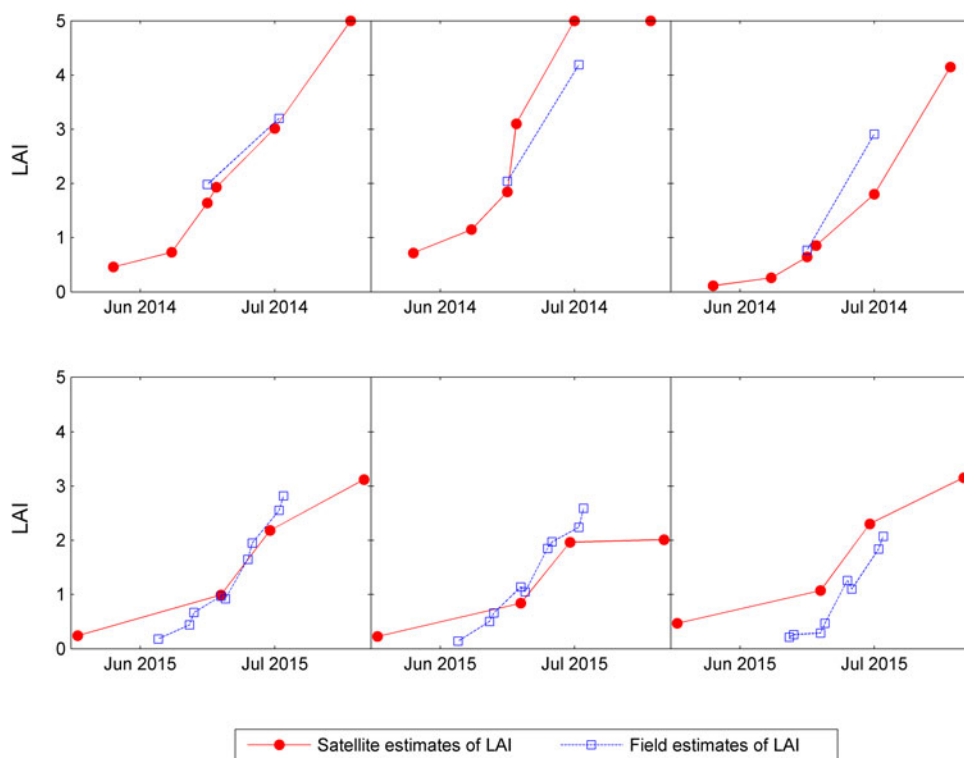


**Fig. 5.** Time evolution of LAI estimates from satellite images and ground measurements at three of the selected maize fields of Improsta farm (top row) and Soffritti farm (bottom row).

**Table 1.** Overview of the methods employed in the performance analysis

Approach	LAI	Weather data source
IRRISAT	Last available image	COSMO-LEPS
Mixed	Interpolated LAI	COSMO-LEPS
Best estimate	Interpolated LAI	Ground AWS

Figure 6 shows a sample temporal evolution of the 5-day cumulative  $ET_p$  with lead time of 5 days as predicted by IRRISAT, in comparison with the best estimate and the estimate given by the mixed approach (COSMO + interpolated LAI), at two representative test sites located, respectively, at Improsta (left panel) and Soffritti (right panel). The IRRISAT and mixed approaches provided very similar estimates at Improsta in 2014 because of the high frequency of available satellite estimates of LAI. The main reason for dissimilarity between IRRISAT estimates and the best estimates is due to errors in the weather forecasts: on average, IRRISAT underestimates the 5-day cumulative  $ET_p$ . On the contrary, at Soffritti in 2015, IRRISAT overestimated the 5-day cumulative  $ET_p$  compared with the best estimate. Then, in this case, because of less frequent available satellite estimates of LAI, the differences between the estimates given by IRRISAT and mixed approaches were more evident and, as expected, IRRISAT underestimated the 5-day cumulative  $ET_p$  with respect to the results of the mixed approach. The main sources of error in forecasting  $ET_p$  were still due to errors in the weather forecasts, although errors due to LAI approximations were not negligible.

Figures 7(a) and (b) depict the BIAS and RMSE, respectively, of the cumulative  $ET_p$  forecast by IRRISAT with respect to the best estimate. The boxplots show the BIAS and RMSE across all test sites, belonging to the two different farms, for increasing cumulative forecasting time intervals (1, 3 and 5 days). On each box, the central mark is the median, the edges of the box are the 25th and 75th percentiles, the whiskers extend to the most extreme data values not considered outliers, and outliers are plotted individually. The points are drawn as outliers if they are larger than  $q_3 + 1.5(q_3 - q_1)$  or smaller than  $q_1 - 1.5(q_3 - q_1)$ , where  $q_1$  and  $q_3$  are the 25th and 75th percentiles, respectively. The circle mark represents the mean value among all test sites in the same farm.

At Improsta, there was a prevailing negative BIAS, which means that IRRISAT on average underestimated the cumulative

$ET_p$ . At Soffritti, the BIAS was on average positive, indicating overestimation. Table 2 summarizes the average BIAS and RMSE of the forecast  $ET_p$  for different lead times (i.e. 1, 3 and 5 days) at both Improsta and Soffritti farms. The RMSE values were higher for the field sites at Soffritti than those at Improsta, probably because of the combined effect of the errors in weather forecasts and in the LAI approximations, as mentioned above.

The ratio, rBIAS, between the bias in  $ET_p$  due only to the approximations made on LAI and the bias in  $ET_p$  due only to weather forecasts, is defined as follows:

$$rBIAS = \frac{\sum_{i=1}^n |ET_p^{IRRISAT} - ET_p^{MIXED}|}{\sum_{i=1}^n |ET_p^{MIXED} - ET_p^{BEST}|} \quad (8)$$

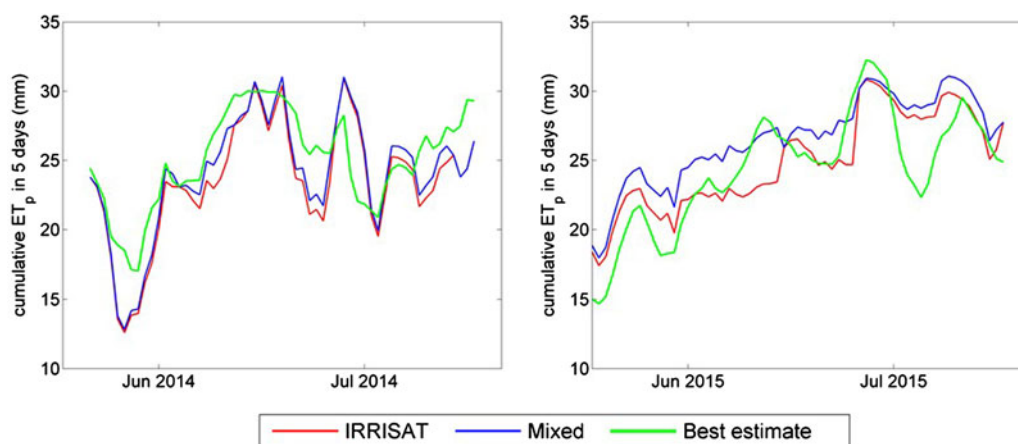
where  $n$  is number of days in the irrigation season.

Figure 8 shows rBIAS across all test sites, belonging to the two different farms, for varying cumulative intervals having increasing lead times (1, 3 and 5 days). Table 2 reports the average rBIAS for different forecast lead times and at both Improsta and Soffritti farms.

The ratio rBIAS was always lower than unity, which means that, for the  $ET_p$  forecasts, the main source of error is given by weather forecasts. It was higher at Soffritti than Improsta because of the less frequent available satellite LAI estimates (Fig. 5), which led to major approximations on LAI values. The variability of rBIAS with the lead time indicates that for Improsta, the impact on forecast errors of the approximations made on LAI increased with the cumulative time interval. For the case of Soffritti, this was valid only for rBIAS related to the 5-day cumulative  $ET_p$ .

## Discussion

Irrigation advisory services can take advantage of the latest generation of high-resolution NWP models, also known as limited area models (LAM), which represent a good data source for retrieving the weather data relevant for  $ET_p$  estimation where the spatial density of weather stations is poor. These models also provide reliable forecasts of weather variables a few days in advance and with a spatial resolution of a few kilometres. In contrast, quantitative forecast of rainfall patterns is still affected by large uncertainty, especially for forecasting lead times longer than 24 h.



**Fig. 6.** Sample time series of 5 days accumulated  $ET_p$  forecasted with a lead time of 5 days by means of the IRRISAT approach and the mixed approach, based on post-processed COSMO-LEPS outputs. The forecasted values are compared with the best estimate obtained by employing measured weather data.

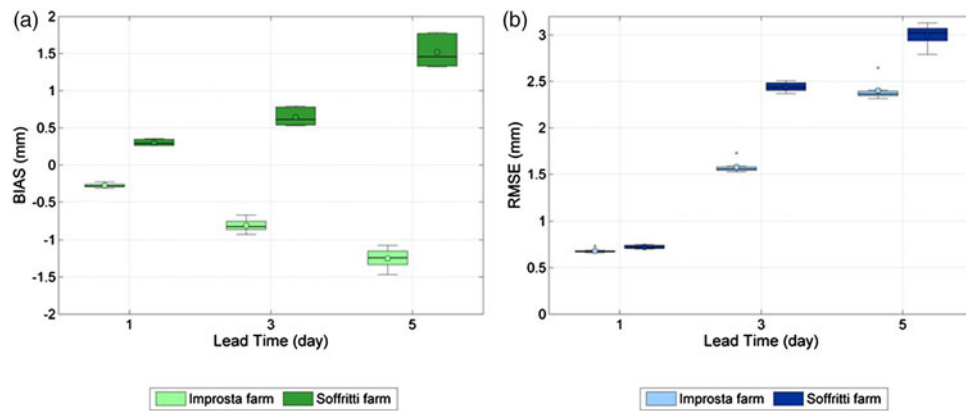


Fig. 7. (a) BIAS (mm) and (b) RMSE (mm) of forecasted  $ET_p$  accumulated in 1, 3 and 5 days for increasing lead time.

The current paper presents the performance of an innovative system providing forecasts of crop  $ET_p$  with a lead time of 5 days, which has been implemented in the IRRISAT irrigation advisory service in Campania region (southern Italy). The forecasting system takes advantage of EO-imagery for assessing crop canopy parameters and a high-resolution NWP model for forecasting weather variables. It combines LAM outputs with a post-processing procedure of the crop VIS-NIR imagery, for computing maps of crop  $ET_p$  based on the Penmann–Monteith equation. Other irrigation services, such as the Irrigation Water Management by Satellite and SMS system (IrriSatSMS) currently implemented in Australia, exploit the NWP model, but they implement the so-called FAO-56 two-steps procedure (Hornbuckle *et al.* 2009). In IrriSatSMS, for example, NWP model outputs are used for forecasting reference crop evapotranspiration ( $ET_0$ ). Earth observation-imagery is then exploited for computing the basal crop coefficient, which is used to scale the forecast  $ET_0$  according to the specific crop phenological state.

Performances of the proposed  $ET_p$  forecasting system were evaluated at two farms in the Campania region, located in areas characterized by significantly different topographic conditions. Potential evapotranspiration forecasts accumulated over 5 days were delivered 5 days in advance with an RMSE <3 mm (i.e. 0.6 mm/day) and an absolute bias <2 mm (i.e. 0.4 mm/day). Local terrain properties greatly affected both reliability of the weather forecasts and accuracy of the canopy parameters estimated from satellite images. In hilly and mountainous areas, weather forecasts are more prone to errors since numerical models (having

a spatial resolution of a few kilometres) are not able to resolve the terrain effects on local weather patterns. Complex terrain features also represent a detrimental factor for post-processing satellite images (Moran *et al.* 1997). For this reason,  $ET_p$  forecast performances at Soffritti, which is located in a hilly area, were generally worse than at Improsta, located in a large river plain.

Another source of error for  $ET_p$  forecasts lies in the fact that crop parameters are updated only when a new satellite image of the crop is available. This means that the accuracy of  $ET_p$  forecasts is influenced by the frequency of satellite acquisitions, especially during the stages of fast crop canopy development. In the current study, the impact of this approximation on the  $ET_p$  forecast was lower than that of the weather forecast errors. Nevertheless, the new EO systems, such as Sentinel-2, can contribute towards lessening the impact of this approximation by providing crop imagery with a smaller repeat cycle. Another option for dampening this source of error is to develop methods for forecasting the crop parameters (Medina *et al.* 2014a). For instance, crop models emulating the dynamic evolution of crop parameters could be implemented by sequentially assimilating the observations provided by satellite images (Chirico *et al.* 2014; Medina *et al.* 2014b).

Besides the valuable forecasting performances, the success of an irrigation advisory service also relies on its usability. For this

Table 2. Summary of the average performance statistics of IRRISAT cumulative  $ET_p$  forecasts with respect to the best estimate

		Forecast lead time		
		1 day	3 days	5 days
Average BIAS (mm)	Improsta farm	-0.28	-0.81	-1.30
	Soffritti farm	0.30	0.64	1.50
Average RMSE (mm)	Improsta farm	0.68	1.60	2.40
	Soffritti farm	0.72	2.40	3.00
Average rBIAS	Improsta farm	0.18	0.23	0.27
	Soffritti farm	0.36	0.39	0.42

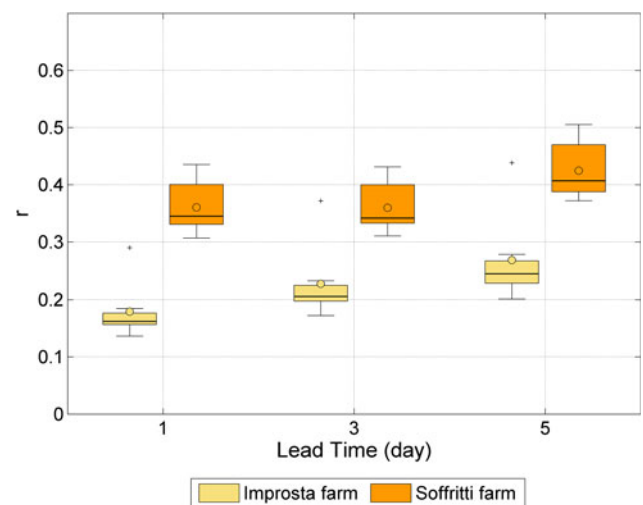


Fig. 8. Ratio between the  $ET_p$  absolute bias due to LAI approximations and the  $ET_p$  absolute bias due to weather forecast errors.

reason, the new ET<sub>p</sub> forecasting system has been integrated with the most advanced web 2.0 technologies to deliver irrigation advice to farmers in an effective and intuitive format. Future studies will be devoted to evaluating the performance of the proposed irrigation advisory service from the end-users' perspective.

**Acknowledgements.** The study is part of the PIRAM project, funded by the European Union and Campania region, within the rural development programme 2007–2013. COSMO-LEPS forecasts were provided by ARPA Emilia Romagna – Servizio Idro-Meteo-Clima. Improsta and Soffritti farms kindly permitted the execution of ground measurements.

## References

- Allen RG, Pereira LS, Raes D and Smith M (1998) *Crop Evapotranspiration – Guidelines for Computing Crop Water Requirements*. FAO Irrigation and Drainage Paper No. 56. Rome, Italy: FAO.
- Allen RG, Pereira LS, Howell TA and Jensen ME (2011) Evapotranspiration information reporting: I. Factors governing measurement accuracy. *Agricultural Water Management* **98**, 899–920.
- Buzzi A, Fantini M, Malguzzi P and Nerozzi F (1994) Validation of a limited area model in cases of Mediterranean cyclogenesis: surface fields and precipitation scores. *Meteorology and Atmospheric Physics* **53**, 137–153.
- Calera A, Campos I, Osann A, D'Urso G and Menenti M (2017) Remote sensing for crop water management: from ET modelling to services for the end users. *Sensors* **17**, article no. 1104. 1–25 doi: 10.3390/s17051104.
- Chirico GB, Medina H and Romano N (2014) Kalman filters for assimilating near-surface observations into the Richards equation – Part 1: retrieving state profiles with linear and nonlinear numerical schemes. *Hydrology and Earth System Sciences* **18**, 2503–2020.
- Clevers JGPW (1989) The application of a weighted infrared-red vegetation index for estimating leaf area index by correcting for soil moisture. *Remote Sensing of Environment* **29**, 25–37.
- Diodato N, Bellocchi G, Romano N and Chirico GB (2011) How the aggressiveness of rainfalls in the Mediterranean lands is enhanced by climate change. *Climate Change* **108**, 591–599.
- D'Urso G (2010) Current status and perspectives for the estimation of crop water requirements from earth observation. *Italian Journal of Agronomy* **5**, 107–120.
- D'Urso G and Calera Belmonte A (2006) Operative approaches to determine crop water requirements from Earth observation data: methodologies and applications. *AIP Conference Proceedings on Earth Observation for Vegetation Monitoring and Water Management* **852**, 14–25. <https://doi.org/10.1063/1.2349323>
- D'Urso G and Menenti M (1995) Mapping crop coefficients in irrigated areas from Landsat TM images. In Engman ET, Guyot G and Marino CM (eds). *Proceedings SPIE 2585, Remote Sensing for Agriculture, Forestry, and Natural Resources*. Paris, France: SPIE, pp. 41–47. doi: 10.1117/12.227167.
- Furcolo P, Pelosi A and Rossi F (2016) Statistical identification of orographic effects in the regional analysis of extreme rainfall. *Hydrological Processes* **30**, 1342–1353.
- GEOSYSTEMS (2017) *ATCOR Workflow for IMAGINE 2016 Version 1.0 Step-by-Step Guide*. Germering, Germany: Geosystems GmbH. Available at [https://www.geosystems.de/fileadmin/redaktion/Software/ATCOR\\_Workflow/ATCOR\\_Workflow\\_for\\_IMAGINE\\_Step\\_by\\_Step\\_Guide.pdf](https://www.geosystems.de/fileadmin/redaktion/Software/ATCOR_Workflow/ATCOR_Workflow_for_IMAGINE_Step_by_Step_Guide.pdf) (Accessed 5 February 18).
- Heinz I (2008) Co-operative agreements and the EU water framework directive in conjunction with the common agricultural policy. *Hydrology and Earth System Sciences Discussions, European Geosciences Union* **12**, 715–726.
- Hornbuckle JW, Car NJ, Christen EW, Stein TM and Williamson B (2009) *IrriSatSMS. Irrigation Water Management by Satellite and SMS – A Utilisation Framework*. CRC for Irrigation Futures Technical Report No. 01/09 and CSIRO Land and Water Science Report No. 04/09. Griffith, NSW, Australia: CSIRO Land and Water.
- LI-COR (1992) *LAI-2000 Plant Canopy Analyzer Instruction Manual*. Lincoln, NE, USA: LiCor Inc. Available at <https://www.licor.com/documents/q6hrj6s79psn7o8z2b2s> (Accessed 18 January 2018).
- Medina H, Romano N and Chirico GB (2014a) Kalman filters for assimilating near-surface observations into the Richards equation – Part 2: a dual filter approach for simultaneous retrieval of states and parameters. *Hydrology and Earth System Sciences* **18**, 2521–2041.
- Medina H, Romano N and Chirico GB (2014b) Kalman filters for assimilating near-surface observations into the Richards equation – Part 3: retrieving states and parameters from laboratory evaporation experiments. *Hydrology and Earth System Sciences* **18**, 2543–2557.
- Montani A, Cesari D, Marsigli C and Paccagnella T (2011) Seven years of activity in the field of mesoscale ensemble forecasting by the COSMO-LEPS system: main achievements and open challenges. *Tellus Series A: Dynamic Meteorology and Oceanography* **63**, 605–624.
- Moran MS, Inoue Y and Barnes EM (1997) Opportunities and limitations for image based remote sensing in precision crop management. *Remote Sensing of Environment* **61**, 319–346.
- Pelosi A and Furcolo P (2015) An amplification model for the regional estimation of extreme rainfall within orographic areas in Campania region (Italy). *Water* **7**, 6877–6891.
- Pelosi A, Medina H, Villani P, D'Urso G and Chirico GB (2016) Probabilistic forecasting of reference evapotranspiration with a limited area ensemble prediction system. *Agricultural Water Management* **178**, 106–118.
- Pelosi A, Medina H, Van den Bergh J, Vannitsem S and Chirico GB (2017) Adaptive Kalman filtering for postprocessing ensemble numerical weather predictions. *Monthly Weather Review* **145**, 4837–4854.
- Pereira LS, Cordery I and Iacovides I (2009) Water scarcity concepts. In Pereira LS, Cordery I and Iacovides I (eds). *Coping with Water Scarcity: Addressing the Challenges*. Dordrecht, The Netherlands: Springer, pp. 7–24.
- Preti F, Forzieri G and Chirico GB (2011) Forest cover influence on regional flood frequency assessment in Mediterranean catchments. *Hydrology and Earth System Sciences* **15**, 3077–3090.
- Richter R (1996) A spatially adaptive fast atmospheric correction algorithm. *International Journal of Remote Sensing* **17**, 1201–1214.
- Romano N, Palladino M and Chirico GB (2011) Parameterization of a bucket model for soil-vegetation-atmosphere modeling under seasonal climatic regimes. *Hydrology and Earth System Sciences* **15**, 3877–3893.
- Stöckle CO (2001) *Environmental Impact of Irrigation: a Review*. Pullman, WA, USA: State of Washington Water Research Center, Washington State University.
- United Nations World Water Assessment Programme (2016) *Water and Jobs*. World Water Development Report 2016. Paris, France: UNESCO. Available at <http://unesdoc.unesco.org/images/0024/002439/243938e.pdf> (Accessed 18 January 2018).
- Vanino S, Pulighe G, Nino P, De Michele C, Falanga Bolognesi S and D'Urso G (2015) Estimation of evapotranspiration and crop coefficients of tendone vineyards using multi-sensor remote sensing data in a Mediterranean environment. *Remote Sensing* **7**, 14708–14730.
- Vuolo F, Neugebauer N, Bolognesi SF, Atzberger C and D'Urso G (2013) Estimation of leaf area index using DEIMOS-1 data: application and transferability of a semi-empirical relationship between two agricultural areas. *Remote Sensing* **5**, 1274–1291.
- Vuolo F, D'Urso G, De Michele C, Bianchi B and Cutting M (2015) Satellite-based irrigation advisory services: a common tool for different experiences from Europe to Australia. *Agricultural Water Management* **147**, 82–95.
- WMO (2012) *Guide to Agricultural Meteorological Practices*. 2010 Edition, updated 2012. WMO No. 134. Geneva, Switzerland: WMO.
- Wriedt G, Van der Velde M, Aloe A and Bouraoui F (2009) Estimating irrigation water requirements in Europe. *Journal of Hydrology* **373**, 527–544.
- Zoccatelli D, Borga M, Chirico GB and Nikolopoulos EI (2015) The relative role of hillslope and river network routing in the hydrologic response to spatially variable rainfall fields. *Journal of Hydrology* **531**, 349–359.